Metal Ion Substitution at the Catalytic Site of Horse-Liver Alcohol Dehydrogenase: Results from Solvent Magnetic Relaxation Studies. 2. Binding of Manganese(II) and Competition with Zinc(II) and Cadmium(II) Ions†

Inger Andersson, Wolfgang Maret, Michael Zeppezauer,* Rodney D. Brown, III, and Seymour H. Koenig*

ABSTRACT: The interaction of Mn^{2+} aquo ions with native horse-liver alcohol dehydrogenase demetalized specifically at the catalytic sites has been investigated by studying the magnetic field dependence and time dependence of the magnetic spin–lattice relaxation rate of solvent water protons. We find no detectable binding of Mn^{2+} ions to the catalytic sites in times on the order of hours; however, we do find that these ions bind to the enzyme at two previously unreported types of sites: one, characterized by a low dissociation constant (0.01 mM at pH 7.7, 5 °C), low relaxivity, and a stoichiometry of one per two catalytic sites, and a second, with a high dissociation constant (1.5 mM at pH 7.7, 5 °C) and high relaxivity. The stoichiometry of the second type of site could not be determined because of the relatively weak binding of Mn^{2+} ions to these sites. Both Zn^{2+} and Cd^{2+} ions bind to the newly found tight-binding sites, displacing Mn^{2+} ions and thereby altering the relaxation rates of solvent protons. By monitoring the return to equilibrium of these altered rates, we find that Zn^{2+} ions enter the catalytic sites from the new tight-binding sites with an on-rate of $\sim 0.1\ M^{-1}\ s^{-1}$. It is not clear whether binding to these new sites is an obligatory intermediate for reintroduction of Zn^{2+} ions into the catalytic sites, but a small excess of Zn^{2+} ions beyond one per monomer causes the protein to precipitate. Cd^{2+} ions, by contrast, enter the catalytic sites at least 1 order of magnitude more rapidly than do Zn^{2+} ions, a rate too rapid to observe by our techniques. However, once the catalytic sites are filled, Cd^{2+} ions displace Mn^{2+} ions at the new sites as do Zn^{2+} ions.

By monitoring changes in the NMRD[1] spectra of solutions of apo(c)Zn(n)-ADH[1] as Mn^{2+} ions were added, we found two distinct types of binding sites for Mn^{2+} ions. Zn^{2+} and Cd^{2+} ions were introduced subsequently to compete with the Mn^{2+} ions at these sites; the resulting time dependence of the NMRD spectra showed that these Mn^{2+}-binding sites differ from the catalytic sites. No detectable amounts of Mn^{2+} ions entered empty catalytic sites in times on the order of hours under our experimental conditions. By contrast, Zn^{2+} and Cd^{2+} ions bind to at least one of these new sites, displacing bound Mn^{2+} ions, but each, with different characteristic rates, ultimately binds strongly to the catalytic sites. As the catalytic sites take up the competing Zn^{2+} or Co^{2+} ions, the displaced Mn^{2+} ions return to their initial distribution.

The technique of NMRD is uniquely suited for studying the kinetics of protein–metal ion interactions of this sort, particularly when one of the ions is Mn^{2+} (which is paramagnetic) and the others are diamagnetic (Koenig et al., 1978). The NMRD spectrum of the Mn^{2+} aquoion is distinctive and qualitatively different from the spectra of all Mn^{2+} macromolecular complexes studied to date. The latter, though similar as a class, are generally site specific [cf. Brown et al. (1977)]. Moreover, the contributions of Mn^{2+} ions at different sites to the overall NMRD spectrum are additive, so that the kinetics of competitive interactions of Mn^{2+} ions with diamagnetic ions can be followed so long as the time scales of interest are no shorter than a few minutes.

Because of the special nature of the interaction of Mn^{2+} ions with ADH and the unique nature of the NMRD of Mn^{2+} ions, the concerns of the present paper are quite different than those of the preceding paper (Andersson et al., 1981); here the interest is the details of the interaction of metal ions with selectively demetalized protein, whereas in Andersson et al. (1981) the interest was the interaction of solvent with reconstituted, remetalized protein.

Experimental Procedures

Materials. The materials used in these experiments derive from the crystalline preparations used in Andersson et al. (1981) and were handled in a similar fashion.[2]

Methods. NMRD measurements are as described in Andersson et al. (1981); all results are for 5 °C. The NMRD spectrum of Mn^{2+} aquo ions is unique among all common free and bound paramagnetic ions (including bound Mn^{2+} ions) in that there is a significant dispersion of the solvent proton spin–lattice relaxation rate at magnetic fields below ~ 0.5 MHz.[3] (This is illustrated in Figure 3.) From a comparison of the difference in relaxation rates between 0.01 and 0.5 MHz of a solution of Mn^{2+} ions and macromolecules with that of a solution of known concentration of Mn^{2+} ions in buffer, it is possible to obtain a quantitative measure of the concentration of Mn^{2+} ions free in solution with a sensitivity of $\sim 5\ \mu M$. Also, for free Mn^{2+} ions, the relaxation rate decreases continuously as the magnetic field is increased. By contrast, Mn^{2+}

† From the Fachbereich 15.2, Analytische und Biologische Chemie, Universität des Saarlandes, Saarbrucken, West Germany (I.A., W.M., and M.Z.) and the IBM Thomas J. Watson Research Center, Yorktown Heights, New York 10598 (R.D.B. and S.H.K.). *Received July 1, 1980; revised manuscript received January 30, 1981.*

[1] Abbreviations used: ADH, horse-liver alcohol dehydrogenase; NMRD, nuclear magnetic relaxation dispersion; NADH and NAD^+, respectively, reduced and oxidized nicotinamide adenine dinucleotide; A(c)B(n)-ADH, enzyme with divalent metal ions of type A in the catalytic sites and divalent metal ions of type B in the noncatalytic sites; Tes, 2-[[tris(hydroxymethyl)methyl]amino]ethanesulfonic acid.

[2] Protein concentration is quoted throughout as molarity of monomer units, though the protein is dimeric.

[3] Magnetic field strength is given in units of the Larmor precession frequency of protons in that field. The conversion is 4.26 KHz = 1 Oe = 1 G.

0006-2960/81/0420-3433$01.25/0

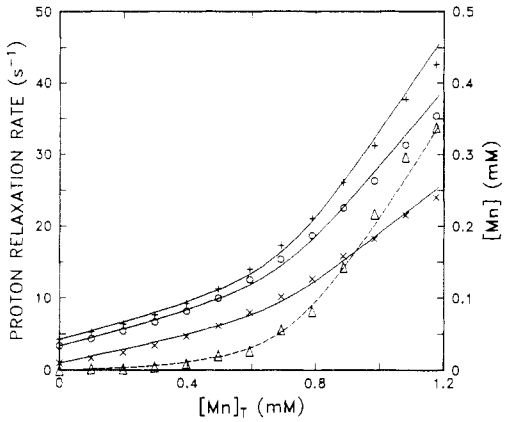

FIGURE 1: Titration of Mn^{2+} ions into 1.65 mM apo(c)Zn(n)-ADH in 0.025 M Tes buffer, pH 7.7, at 5 °C. The solvent proton relaxation rates were measured at 0.01 (+), 0.5 (○), and 20 (×) MHz. The concentration of Mn^{2+} aquo ions (right-hand scale), computed at each value of total added Mn^{2+} ion concentration, $[Mn]_T$, from the differences in relaxation rates at 0.01 and 0.5 MHz, is indicated by (△). The solid curves through the data points and the dashed curve through the aquo ion points were computed by assuming two types of binding sites on the protein: one a tight-binding, low-relaxivity site with dissociation constant K_L = 0.01 mM and relaxivities 10.5 and 8.7 mM^{-1} s^{-1} at the low and high fields, respectively, and the second a weak-binding, high-relaxivity site with dissociation constant K_H = 1.5 mM and analogous relaxivities of 106 and 100 mM^{-1} s^{-1}. The stoichiometry of low-relaxivity sites is 0.85 per dimer of protein (see text) for the best fit of the data to this model; the stoichiometry of high-relaxivity sites was taken as one per dimer, but the binding is too weak to determine the true stoichiometry of these sites.

macromolecular complexes generally have a peak in their NMRD spectra in the range 10–50 MHz [the origin of which is well understood; cf. Koenig et al. (1973)], with a maximum relaxivity (relaxation rate per unit concentration of paramagnetic ion) often 1 order of magnitude or more greater than that of aquo ions at similar fields. Thus, measurements at two low fields give the concentration of free Mn^{2+} ions, and measurements at a single high field yield information on the distribution of the bound ions.

Results and Analysis

Titration of Mn^{2+} Ions. Figure 1 shows the results of a titration of Mn^{2+} ions into 1.65 mM apo(c)Zn(n)-ADH in 0.025 M Tes buffer, pH 7.7, at 5 °C. The data were taken at three values of magnetic field: 0.01, 0.5, and 20 MHz. No time-dependent drifts of the relaxation rates after addition of Mn^{2+} ions were observed, even after several hours of monitoring selected samples. The differences between the data points at 0.01 and 0.5 MHz (corrected for a small difference due to the demetalized protein in the absence of added Mn^{2+} ions) are a measure of the concentration of Mn^{2+} aquo ions; the triangles show the variation of the concentration of Mn^{2+} aquo ions as a function of total added Mn^{2+} ions derived from the data for 0.01 and 0.5 MHz.

Three qualitative features are immediately clear from the data of Figure 1: (1) the concentration of Mn^{2+} aquo ions is a very small fraction of the total until ~0.6 mM total Mn^{2+} ions have been added; (2) even at the maximum concentration of total Mn^{2+} ions used, only a part of the incrementally added ions remain free in solution; (3) there must be (at least) two different types of binding sites for Mn^{2+} ions, judging from the upward curvature of the 20 MHz data as free Mn^{2+} ions begin to appear in solution. (The last conclusion assumes no allosteric or cooperative interactions upon binding of two Mn^{2+} ions per dimer in equivalent sites.)

Quantitatively, the data can be fit by assuming one Mn^{2+}-binding site per active dimer (see below) with a low

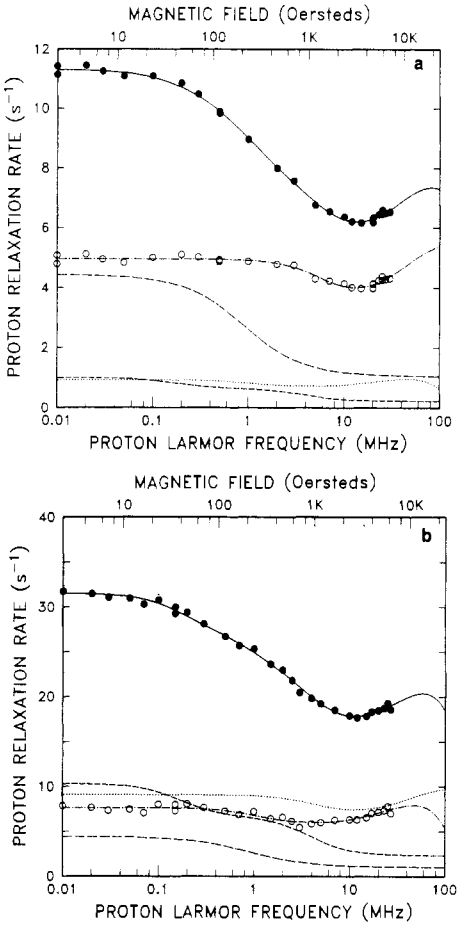

FIGURE 2: (a) (●) NMRD spectrum of solvent protons for a sample with 0.5 mM total Mn^{2+} ions added to 1.54 mM apo(c)Zn(n)-ADH in 0.025 M Tes buffer, pH 7.7, at 5 °C. The major paramagnetic contribution to the spectrum is from Mn^{2+} ions bound in the low-relaxivity sites (cf. Figure 1). The contributions to the total spectra (obtained from other data) are shown for apo(c)Zn(n)-ADH (– – –), Mn^{2+} aquo ions (---), and Mn^{2+} ions bound in the high-relaxivity sites (···). The data, corrected for these contributions, give the NMRD spectrum of the low-relaxivity sites, which is shown by (○). The curve through these points (–·–) is from a least-squares comparison of the data with the usual theory of relaxation. (b) Analogous to (a) except that 1.0 mM total Mn^{2+} ions were added so that the total NMRD spectrum (●) contains a significant contribution from the high-relaxivity sites, indicated by (○). Here, (···) is the contribution of the low-relaxivity sites and (–·–) is the fit to the high-relaxivity site dispersion.

dissociation constant and relatively low relaxivity and a second site with a significantly greater dissociation constant and a higher relaxivity. (The data are insufficient to determine whether the stoichiometry of the high-relaxivity site is one per dimer or one per monomer; we assume the former.) The solid lines through the data points result from a fit to the data using K_L = 0.01 mM and K_H = 1.5 mM for the dissociation constants of Mn^{2+} ions from the low- and high-dissociating sites, respectively. Values for the relaxivities of Mn^{2+} ions in the low-relaxivity sites were obtained from the slope of the data in Figure 1, in the limit of low total concentration of Mn^{2+} ions, as was the value of K_L. Values of relaxivities of Mn^{2+} ions in the high-relaxivity sites were obtained by iteration, estimating values of relaxivity and K_H that gave a reasonable description of the data, and then refining these values to optimize the fit. It is quite clear, from Figure 1, that a model with two types of sites, one with a relatively low dissociation constant, low relaxivity, and a stoichiometry of one per dimer and a second with a relatively high dissociation constant and high relaxivity, is adequate to describe the titration data within

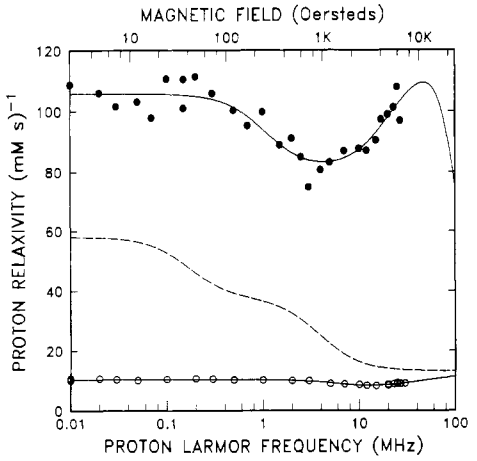

FIGURE 3: Comparison of contributions to solvent proton relaxation, expressed in units of relaxivity, of low-relaxivity sites (○), high-relaxivity sites (●), and Mn^{2+} aquo ions (---) for the specific solvent conditions used here.

the experimental uncertainties. That neither of these sites is the catalytic site is demonstrated below.

NMRD Spectra of the Two Types of Sites. Figure 2a shows the NMRD spectra of a sample with a sufficiently low total concentration of Mn^{2+} ions so that the bound ions are essentially all at low-relaxivity sites. The upper set of point shows the raw data; the lower set of points shows the data corrected for the contributions to the relaxation rates of the Mn^{2+} aquoions, Mn^{2+} ions bound at the high relaxivity site, and the enzyme demetalized at the catalytic site, obtained from Andersson et al. (1981). The line through the corrected data points results from a least-squares comparison of the data with the theory of relaxation by paramagnetic ions, as described previously (Brown et al., 1977). The most important parameter of the theory, for the present purposes, is τ_M, the residence lifetime of an assumed single exchaning water ligand of the bound Mn^{2+} ions, which we find to be 1.4 μs.

Part b of Figure 2 is analogous to part a except that the total concentration of Mn^{2+} ions is greater, so that the contributions to the relaxation rates from ions in the two types of sites are roughly equal. The exact contribution from each type of site depends on its fractional occupancy; these were computed by using the values for K_L and K_H obtained from the analysis of the data of Figure 1. The result for τ_M for the high-relaxivity site is 0.2 μs.

Figure 3 shows a comparison of the NMRD spectra of the two types of sites obtained from Figure 2a,b, expressed in units of relaxivity. The difference between the two curves is accounted for almost entirely by the difference in the τ_M of the water ligand of the bound Mn^{2+} ions at the two types of sites. Also shown is the relaxivity spectrum for Mn^{2+} aquo ions at the same temperature to illustrate the relative contributions of Mn^{2+} ions for each of the three conditions. (It should also be pointed out that there can be a large systematic error in the magnitude of the relaxivity of the high-relaxivity sites because the number of ions bound to these sites has a large uncerainty; it depends on the difference of two comparable quantities, the total added Mn^{2+} ions and the number elsewhere.)

Displacement of Mn^{2+} Ions by Zn^{2+} Ions. A series of experiments was performed on a solution of 1.60 mM apo(c)-Zn(n)-ADH that had been equilibrated with a 0.5 mM total concentration of added Mn^{2+} ions. Essentially all of the Mn^{2+} ions were bound under these conditions. Successive increments of Zn^{2+} ions were then added, for respective totals of 0.25, 0.75, 1.25, and 1.75 mM, and the relaxation rates at 0.01, 0.5, and

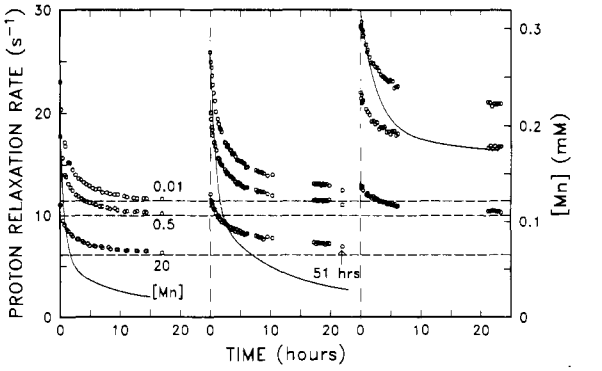

FIGURE 4: Solvent proton relaxation rates as a function of time after addition of successive increments of Zn^{2+} ions to a sample of 1.60 mM apo(c)Zn(n)-ADH (monomer concentration) in 0.025 M Tes buffer, pH 7.7, to which 0.5 mM total Mn^{2+} ions and 0.25 mM Zn^{2+} ions were previously added. The three curves show data of 0.01, 0.5, and 20 MHz after, from left to right, three subsequent additions of 0.5 mM Zn^{2+} ions (for a total of 1.75 mM Zn^{2+} ions). The three dashed horizontal lines show the measured relaxation rates in the absence of any added Zn^{2+} ions. The solid lines show the time dependence of the concentration of the Mn^{2+} aquo ions (right-hand scale) obtained by fitting a smooth curve to the differences between the 0.01- and 0.5-MHz data.

20 MHz were monitored as a function of time after each addition. The time-dependent changes after the first addition were too rapid to monitor effectively; the data for the three subsequent additions are shown in Figure 4.

The results for the second and third additions (Figure 4) are essentially identical except for the time scale: there is an initial increase in the relaxation rates at the three fields shown, with a significant increase in the concentration of Mn^{2+} aquo ions; the final relaxation rates return to the same values in each case, equal to that observed before any addition of Zn^{2+} ions, as indicated by the dashed horizontal lines (cf. Figure 1). However, the slopes of the initial decays differ by a factor of $\sim$1.5, corresponding to a slower decay after the third addition than after the second. (The differences in the relaxation rates at "zero" time are instrumental and result from the faster decay of the left-most set of curves and the limitations of the time resolution of the apparatus.) Qualitatively, these data are consistent with the conjecture that the Zn^{2+} ions initially displace some Mn^{2+} ions from the tight-binding, low-relaxivity sites and then slowly "disappear" into sites inaccessible to the Mn^{2+} ions (the catalytic sites). Quantitatively, this initial displacement is near stoichiometric when the unfilled low-relaxivity sites are accounted for, indicating that the binding of Zn^{2+} ions to these sites is significantly stronger than that of Mn^{2+} ions. The values of the relaxation rates immediately after the incremental addition of 0.5 mM Zn^{2+} ions correspond to the rates expected on the basis of the binding constants and relaxivity values deduced from Figure 1 when the effect of the added Zn^{2+} ions is considered as reducing, stoichiometrically, the number of low-relaxivity sites.

The results in Figure 4 after the fourth addition of Zn^{2+} ions (the right-most set of results) are the only ones for which the total concentration of Zn^{2+} ions is greater than that of the catalytic sites. In this case, again qualitatively, the initial changes in relaxivity correspond, as before, to a displacement from the low-relaxivity sites of an equivalent amount of Mn^{2+} ions, but now, because of the excess of Zn^{2+} ions, there is a permanent displacement of the Mn^{2+} ions to a new distribution, with more in the weak-binding, high-relaxivity sites and more free. A detailed analysis of the stoichiometry of the data in Figure 4, using the relaxivity values from Figure 1, indicates that the number of catalytic sites that are filled by the Zn^{2+}

ions is ~89% of the number of monomeric units. This compares well with the results of Maret et al. (1979), who measured the concentration of active sites by titration of coenzyme [cf. Einarsson et al. (1976)] and typically found it to be close to 85% of the total protein concentration as measured by optical absorption. [It appears that 85% availability of active enzyme in preparations of ADH from commercial sources is typical (M. Zeppezauer, unpublished observations).] Thus, for the fourth addition of Zn^{2+} ions (Figure 4), the final state of the sample is 1.35 mM Zn^{2+} ions bound at the catalytic sites, 0.40 mM Zn^{2+} ions bound in the low-relaxivity sites, and the 0.5 mM Mn^{2+} ions distributed among the remainder of these latter sites, the high-relaxivity sites, and in solution in a manner that can be computed from K_L, K_H, and the difference in the 0.01 and 0.5 MHz rates by assuming one high-relaxivity site per available active site.

An important point to note in the foregoing experiments is that the total concentration of Mn^{2+} ions is about one-third that of protein monomers. Nonetheless, incremental addition of the same concentrations of Zn^{2+} ions produces a transient displacement of Mn^{2+} ions to other sites on the protein, indicating that all the low-relaxivity sites are saturated by less than two-thirds monomer equivalent of metal ions. This is consistent with the conclusions from the titration data (Figure 1) that the stoichiometry of these sites is one per two monomers.

A rudimentary theoretical description of the initial time dependence of the relaxation rates, for the concentrations used in Figure 4, can be derived if it is assumed that the rate-limiting step in the kinetics is the binding of Zn^{2+} ions to the catalytic sites from the reservoir of other, nonspecific, sites and/or from solution. The rate of change of the concentration of these available Zn^{2+} ions is

$$\frac{d}{dt}[Zn_{avail}] = -k[Zn_{avail}]([P_I] - [Zn_T] + [Zn_{avail}]) \quad (1)$$

Here $[P_I]$ is the concentration of unfilled catalytic sites just before the incremental addition of Zn^{2+} ions, $[Zn_T]$ is the total concentration of incrementally added Zn^{2+} ions, and k is a second-order rate constant that describes the rate-limiting recombination step at the catalytic site. The expression $[P_I] - [Zn_T] + [Zn_{avail}]$ is the number of unoccupied catalytic sites at any particular time and, of course, can never become negative.

The differential equation, eq 1, is identical in form to that describing analogous kinetics of metal ion substitution in concanavalin A (Koenig et al., 1978), and a detailed discussion of the exact solution, valid for all times, can be found there. However, the short-time and long-time behaviors of the solutions are straightforward to analyze. At short times, essentially all the incrementally added Zn^{2+} ions are available, and their concentration will initially decay exponentially with a time constant equal to $(k[P_I])^{-1}$, whether or not $[Zn_T]$ is in excess of $[P_I]$. Thus, the more catalytic sites are initially filled, the smaller is $[P_I]$ and the slower is the decay of the available Zn^{2+} ions. For long times, $[Zn_{avail}] \rightarrow 0$ if $[P_I] - [Zn_T] \geq 0$, and approaches $[Zn_T] - [P_I]$ otherwise. The decay in this limit is also exponential with a time constant $(k|[P_I] - [Zn_T]|)^{-1}$ proportional to the number of catalytic sites that remained unfilled after a long time in the first case and to the excess in the other.

If it is assumed that the Mn^{2+} ions progressively return to the sites from which they were displaced as the Zn^{2+} ions recombine at the catalytic sites, then the time dependence of the concentration of free Mn^{2+} ions simply reflects the kinetics of the binding of the Zn^{2+} ions. This assumption holds during the fast part of the decays in Figure 4, when there are sufficient Zn^{2+} or Mn^{2+} ions available to essentially saturate the low-dissociating sites; then, because the binding of Mn^{2+} ions to the remaining sites is weak, the concentration of free ions is proportional to the total displaced from the low-relaxivity sites. For longer times, empty low-relaxivity sites occur and, since the binding of Mn^{2+} ions to these sites is not infinitely strong, the concentration of free Mn^{2+} ions approaches its long-time value very slowly. The solid curves show the decay of the Mn^{2+} aquo ion concentration as a function of time, obtained initially from the differences in the relaxation rates at 0.01 and 0.5 MHz. The progressive slowing of the initial decay rates seen in Figures 4 correlates qualitatively with the progressively smaller value of $[P_I]$.

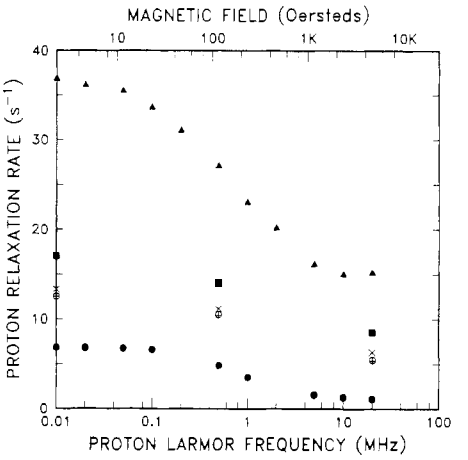

FIGURE 5: NMRD spectra of a sample of 2.38 mM apo(c)Zn(n)-ADH in 0.025 M Tes buffer, pH 7.7, 5 °C (●) to which first 0.5 mM Mn^{2+} ions were added (+) and then totals of 0.75 mM (○), 2.25 mM (×), and 2.55 mM (■) Cd^{2+} ions and finally 0.5 mM Zn^{2+} ions (△) were added.

Displacement of Mn^{2+} Ions by Cd^{2+} Ions. The phenomena observed upon addition of Cd^{2+} ions are similar to those observed with Zn^{2+} ions, except that Cd^{2+} ions enter the catalytic sites at rates too fast to be observed. This is demonstrated in Figure 5. The lowest data points show the NMRD spectra for a sample of 2.38 mM apo(c)Zn(n)-ADH before addition of any metal ions. Data for 0.01, 0.5, and 20 MHz are shown after addition of 0.5 mM Mn^{2+} ions, then 0.75 mM total Cd^{2+} ions, and then additional increments for a total of 2.25 mM Cd^{2+} ions. The presence of this concentration of Cd^{2+} ions has, as seen, no significant effect on the relaxation rates. Addition of 0.3 mM Cd^{2+} ions more, for a total of 2.55 mM Cd^{2+} ions, increases the relaxation rates at all fields significantly. Finally, 0.5 mM Zn^{2+} ions were added to the sample. The NMRD spectra for this situation is shown at the top of Figure 5. The data, which were independent of time for many hours, indicate that the Zn^{2+} ions displaced a sizable fraction of the Mn^{2+} ions and that the majority, ~0.4 mM, are aquo ions.

Qualitatively, the results shown in Figure 5 can be explained as follows. The 0.5 mM of Mn^{2+} ions bind to the low-relaxivity sites, of which there are nominally 1.2 mM (one per dimer). As Cd^{2+} ions are added, they enter the catalytic sites in a time too short to be seen in the present experiments and therefore do not induce a time-dependent relaxation rate as does addition of Zn^{2+} ions. Neither do they alter the relaxation rate at all until they fill the catalytic sites plus a number of low-relaxivity sites sufficient for a small number of Mn^{2+} ions to be displaced to the high-relaxivity sites; addition of 2.55 mM Cd^{2+} ions is seen to suffice in the present case. This requires a stoichiometry of active sites equal to ~82% of the monomer

concentration (determined by optical absorption). The computed excess concentration of Cd^{2+} ions, 0.6 mM, together with a 0.5 mM added concentration of Zn^{2+} ions is sufficient to occupy over 90% of the 1.0 mM low-relaxivity sites. The 0.5 mM Mn^{2+} ions can then be computed to partition with ~0.35 mM free in solution, with the remainder shared roughly equally by the two types of sites. This can be shown to give relaxivities at the different fields in good agreement with the data (Figure 5).

Ion-Induced Polymerization. It was our experience, and that of others (e.g., Maret et al., 1978), that apo(c)Zn(n)-ADH tended to precipitate in solution in the presence of added Zn^{2+} ions, and the idea developed that the presence of Zn^{2+} ions in the low-relaxivity sites, of which there is one per dimer, might lead to tetramerization, subsequent polymerization, and ultimately precipitation. First, 2.0 mM Zn^{2+} ions were added to a solution of 2.4 mM apo(c)Zn(n)-ADH; then the concentration of Zn^{2+} ions was increased to 2.5 mM and finally to 3 mM. The relaxation rates were monitored at several fields. The relaxation rate at 0.01 MHz increased by ~10% immediately after the first addition of Zn^{2+} ions, returning to the apo(c)Zn(n)-ADH value with a time constant of ~10 min. There were no significant changes above 0.5 MHz. Subsequent addition of 0.5 mM Zn^{2+} ions produced similar time-dependent changes that were about twice the magnitude of the previous change. Addition of another 0.5 mM Zn^{2+} ions, for a total of 3.0 mM, produced irreversible changes. Initially, the relaxation rate at 0.01 MHz increased by 50%, at 0.1 MHz by 25%, and at fields above 0.5 MHz not at all. Within ~2 hours, after a slight decrease, the relaxation rates at 0.01 and 0.2 MHz had increased another 50–100% and thereafter increased very rapidly. The sample, then removed from the apparatus, was turbid, indicating significant precipitation.

Discussion

The main result of the present work is the discovery of a metal-binding site on ADH molecules, other than the catalytic and noncatalytic sites, for which the dissociation constant of Mn^{2+} ions is small, ~0.01 mM at 5 °C and pH 7.7, and significantly smaller for Zn^{2+} and Cd^{2+} ions. The relaxivity of Mn^{2+} ions in this site is relatively low. The stoichiometry is very close to one per two catalytic sites. The latter, for the present enzyme preparations, averages ~0.85 per protein monomer, typical of earlier experiences under other circumstances (Maret et al., 1979).

We also have found (at least) one additional type of binding site for Mn^{2+} ions characterized by relatively weak binding (dissociation constant ~1 mM) and high relaxivity. The stoichiometry of these sites is as yet undetermined, as is the extent of binding of Zn^{2+} and Cd^{2+} ions to these sites. Moreover, the binding of Mn^{2+} ions at both types of sites is unaffected by the presence or absence of Zn^{2+} or Cd^{2+} ions at the catalytic sites.

Zn^{2+} ions added to solutions of apo(c)Z(n)-ADH, so long as they are not in excess, bind initially to the new tight-binding sites before going to the catalytic sites. The on-rate k to the catalytic sites (cf. eq 1 and Figure 4) is ~0.1 M^{-1} s^{-1}. We have as yet no indication, however, whether binding at these sites is an obligatory intermediate for binding of Zn^{2+} ions at the catalytic sites or whether these sites act essentially as a reservoir of ions that return to solution as other ions from solution become bound at the catalytic sites. This point is somewhat awkward to investigate since excess Zn^{2+} ions presumably bind to the high-relaxivity sites as well; whether this binding is relatively weak as it is for Mn^{2+} ions or much stronger for Zn^{2+} ions, the observation is that when somewhat over 1 monomer equivalent of Zn^{2+} ions is added to a solution of Zn(c)Zn(n)-ADH, the protein aggregates immediately and, after ~2 h, starts to precipitate.

A related observation has been reported by Maret et al. (1979), who find that precipitation occurs in solutions of apo(c)Zn(n)-ADH into which additional Zn^{2+} ions are introduced by dialysis when the dialyzing solution contains a concentration of Zn^{2+} ion greater than ~20 μM. This concentration is sufficient to saturate all the tight-binding sites (one per dimer) and conceivably a sizable fraction of the weak-binding sites as well if their affinity for Zn^{2+} ions is significantly greater than for Mn^{2+} ions. Conceivably, the one Zn^{2+} ion per dimer in the low-relaxivity sites allows tetramer formation and subsequent polymerization when augmented by the charge introduced by binding of additional metal ions at the high-relaxivity sites.

The behavior of Cd^{2+} ions is similar in all aspects to that of the Zn^{2+} ions, except that the on-rate of Cd^{2+} ions to the catalytic sites is at least 1 order of magnitude greater than that of Zn^{2+} ions. By contrast, the fact that we see no indication that Mn^{2+} ions enter the catalytic site over a period of several hours means that their on-rate, if they bind at all, must be at least 3 orders of magnitude less than that of Zn^{2+} ions.

The correlation found here between the strength of binding and the magnitude of relaxivity has been observed before. For example, addition of Mn^{2+} ions to demetalized concanavalin A results in a weakly bound Mn^{2+}–protein complex that has a high relaxivity (Brown et al., 1977), comparable to that observed here for the high-relaxivity site. The dissociation constant in that case was ~1 mM at pH 5 and a function of pH in a manner that suggested that the dissociation rate of the complex was independent of pH (whereas the rate of formation was influenced by competition with protons). Addition of Ca^{2+} ions to the Mn^{2+}–concanavalin A complex leads to a new equilibrium form for which the rate of dissociation of the Mn^{2+} ions from the protein is limited by the off-rate of the Ca^{2+} ions. This ternary complex has a relaxivity comparable to that found here for Mn^{2+} ions bound to the low-relaxivity, tight-binding sites. Both in concanavalin A and in ADH, the differences between the relaxivities of the low- and high-relaxivity complexes arise from differences in the off-rate of water ligands of the bound Mn^{2+} ions, which in turn correlate with the off-rates of the ions themselves from the respective Mn^{2+}–protein complexes.

Finally, the foregoing is another example of the utility of the NMRD technique as an indicator of change during complexation of proteins with both diamagnetic and paramagnetic metal ions. Here, as in other instances (Brown et al., 1977; Koenig et al., 1978), it has been possible to study the kinetics of fairly complex interactions with high accuracy in situations that are amenable to study by few, if any, other techniques. Moreover, the accuracy of the data and the validity of the conclusions do not depend upon a proper theory for the relaxation effects themselves, a problem that has raised questions regarding the interpretation of other applications of relaxation measurements [cf. Koenig (1978) and Koenig & Brown (1980)].

References

Andersson, I., Maret, W., Zeppezauer, M., Brown, R. D., III, & Koenig, S. H. (1981) *Biochemistry* (preceding paper in this issue).

Brown, R. D., III, Brewer, C. F., & Koenig, S. H. (1977) *Biochemistry 16*, 3883–3893.

Einarsson, R., Widell, L., & Zeppezauer, M. (1976) *Anal. Lett. 9*, 815–823.

Koenig, S. H. (1978) *J. Magn. Reson. 31*, 1-10.
Koenig, S. H., & Brown, R. D., III (1980) in *ESR and NMR of Paramagnetic Species in Biological and Related Systems* (Bertini, I., & Drago, R., Eds.) pp 89-115, D. Reidel, Boston, MA.
Koenig, S. H., Brown, R. D., III, & Brewer, C. F. (1973) *Proc. Natl. Acad. Sci. U.S.A. 70*, 475-479.
Koenig, S. H., Brewer, C. F., & Brown, R. D., III (1978) *Biochemistry 17*, 4251-4260.
Maret, W., Andersson, I., Dietrich, H., Schneider-Bernlöhr, H., Einarsson, R., & Zeppezauer, M. (1979) *Eur. J. Biochem. 98*, 501-512.

Evidence for Two Acyl Group Conformations in Some Furylacryloyl- and Thienylacryloylchymotrypsins: Resonance Raman Studies of Enzyme-Substrate Intermediates at pH 3.0†

B. A. E. MacClement, R. G. Carriere, D. J. Phelps, and P. R. Carey*

ABSTRACT: Resonance Raman (RR) spectra, obtained by ultraviolet laser excitation, are reported for 10 acylchymotrypsins at pH 3.0, in which the acyl groups are derivatives of furylacrylic and thienylacrylic acids. Spectra are also shown of the sodium dodecyl sulfate ($NaDodSO_4$) denatured acyl enzymes and the acid and ester analogues of the acyl groups. For most of the native acyl enzymes, the RR spectral profiles in the carbonyl stretching region suggest that the acyl groups bound to Ser-195 adopt two conformations, which are characterized by having either strong hydrogen bonds to the carbonyl oxygen or a nonbonding hydrophobic environment about the C=O group. It is also likely that in solution the ester and acid analogues of the acyl group adopt more than one conformation about the acryloyl linkages. Thus, the measured spectral parameters, such as the ethylenic double bond stretching frequency $\nu_{C=C}$ in the RR spectra, should be considered as a weighted mean, $\langle\nu_{C=C}\rangle$. For a series of compounds based on a given acyl group a correlation exists between $\langle\nu_{C=C}\rangle$ and the measured absorption maximum $\langle\lambda_{max}\rangle$. Possible explanations are given for the observed changes in $\langle\nu_{C=C}\rangle$ and $\langle\lambda_{max}\rangle$ when the acyl groups bind to the active site. A band appears near 1260 cm^{-1} in the RR spectra of some of the native acyl enzymes; it is not observed in the spectra of the $NaDodSO_4$-treated intermediates or in the spectra of any model compounds.

The study of organic reaction mechanisms is greatly aided by noting the change in reactivity with changing structure of the reagents. This approach has given considerable information on, for example, the electronic structure of transition states and the features that determine reactivity. However, similar approaches to the understanding of enzyme mechanism are much more limited (Jencks, 1969; Fersht, 1977). An important factor restricting their use is that structure–reactivity studies with enzymes tend to measure the effect of changes in the structure of the substrate on its interactions with the enzyme, rather than the effects on the electronic changes in the transition state. In this regard, it may be valuable to have a probe, at the level of atoms and chemical bonds, to independently characterize enzyme–substrate interactions during enzymolysis. The work presented here attempts to explore the possibility of using resonance Raman (RR) spectroscopy to delineate enzyme–substrate interactions within a series of related substrates and thereby isolate the effect of these interactions on kinetic parameters.

The resonance Raman spectrum of a molecule is obtained by using an excitation wavelength for the Raman effect which lies within an electronic absorption band of the molecule. Considerable intensity enhancement of the Raman spectrum is thereby obtained enabling vibrational spectra to be recorded from chromophores in the 10^{-4}–10^{-5} M range. By use of a chromophoric substrate whose absorption lies to the red of normal protein absorption bands, selective enhancement of the substrate vibrational modes, from an enzyme–substrate complex, can be achieved. As a result of the availability of laser wavelengths, the first RR studies on enzyme–substrate intermediates used chromophoric substrates, based on substituted cinnamic acid esters, having an absorption band in the 450-nm region (Carey & Schneider, 1974, 1976). Recent technological advances have made laser lines available in the 325–360-nm spectral range enabling a wider range of substrates, including specific enzyme–substrate intermediates (Storer et al., 1979), to be studied. The 10 substrates considered here are substituted derivatives of furylacrylic and thienylacrylic acids (Figure 1) absorbing in the near-ultraviolet and were chosen and synthesized on the basis of their differing electronic and steric properties. Chymotrypsin is used in this work as a "model" enzyme and was selected on the basis of its availability and known structural and mechanistic properties (Blow, 1976). One of the intermediates studied herein, namely, furylacryloylchymotrypsin has been the object of pioneering studies by absorption spectroscopy (Bernhard & Lau, 1972). Since the reaction of chymotrypsin with acyl imidazoles proceeds via the formation of an acyl enzyme intermediate the rate of breakdown of which is rate determining, it is possible, by manipulating pH and subsequent separation techniques, to obtain a pure stable acyl enzyme at pH 3.0, free from substrate or product. In each acyl enzyme the substrate's acyl group is covalently linked to the side chain of serine-195 in chymotrypsin's active site. This paper is concerned with interpreting the RR spectra of the stable acyl enzymes at pH 3.0 in terms of enzyme–substrate interactions. The following paper (Phelps et al., 1981) deals with those effects most related to kinetic aspects: the effects on the RR spectra of going to active

† From the Division of Biological Sciences, National Research Council of Canada, Ottawa, Canada K1A 0R6. N.R.C.C. No. 19393. *Received October 27, 1980.*

0006-2960/81/0420-3438$01.25/0